DALTON
FULL PAPER

Derivatives of the $[Ru(bipy)(CN)_4]^{2-}$ chromophore with pendant pyridyl-based binding sites: synthesis, pH dependent-luminescence, and time-resolved infrared spectroscopic studies

Susana Encinas,[a] Angeles Farran Morales,[a] Francesco Barigelletti,*[a] Anita M. Barthram,[b] Claire M. White,[b] Samantha M. Couchman,[b] John C. Jeffery,[b] Michael D. Ward,*[b] David C. Grills[c] and Michael W. George[c]

[a] *Istituto FRAE-CNR, Via P. Gobetti 101, 40129 Bologna, Italy. E-mail: franz@frae.bo.cnr.it*
[b] *School of Chemistry, University of Bristol, Cantock's Close, Bristol, UK BS8 1TS.*
E-mail: mike.ward@bristol.ac.uk
[c] *School of Chemistry, University of Nottingham, University Park, Nottingham, UK NG7 2RD.*
E-mail: mike.george@nottingham.ac.uk

Received 3rd July 2001, Accepted 25th September 2001
First published as an Advance Article on the web 26th October 2001

Reaction of $K_4[Ru(CN)_6]$ with 2,2′:4′,4″-terpyridine (L^1) or 2,2′:3′,2″:6″,2‴-quaterpyridine (L^2) in acidic aqueous methanol affords the complexes $K_2[Ru(L^1)(CN)_4]$ and $K_2[Ru(L^2)(CN)_4]$ respectively, both containing the $\{Ru(bipy)(CN)_4\}^{2-}$ chromophore but with pendant pyridyl or bipyridyl units, respectively. Time-resolved IR analysis of $K_2[Ru(CN)_4(L^2)]$ in MeCN–D_2O showed that the most intense CN stretching vibration shifted to higher energy by *ca.* 50 cm^{-1} after laser excitation, consistent with formation of a Ru(III)/$(L^2)^{\bullet -}$ MLCT excited state for which the lifetime measurement (38 ± 5 ns, measured by TRIR) agrees reasonably well with the value measured by luminescence methods (30 ± 2 ns). Study of the pH dependence of the absorption and emission spectra of the two complexes revealed the presence of two different effects arising from protonation of the pendant pyridyl/bipyridyl site (which occurs with $pK_a \approx 3.1$ in each case) and protonation of the cyanide ligands (which occurs with $pK_a \approx 2$ in each case). For $K_2[Ru(L^1)(CN)_4]$, protonation of the pendant pyridyl unit results in the ^{1}MLCT excited state being lowered in energy by *ca.* 1000 cm^{-1}, whereas at lower pH values (2.5–1), protonation of the cyanide ligands raises the ^{1}MLCT excited state energy by over 2000 cm^{-1}. For $K_2[Ru(L^2)(CN)_4]$ in contrast, protonation of the pendant bipyridyl unit has no detectable effect on the ^{1}MLCT energy, as the pendant site is electronically decoupled from the complex core by a substantial twist between the free and coordinated bipy components of L^2; protonation of the cyanides at lower pH values however destabilises the ^{1}MLCT excited state. Protonation of the pendant pyridyl sites results in complete (for $[Ru(L^1)(CN)_4]^{2-}$) or near-complete (for $[Ru(L^2)(CN)_4]^{2-}$) quenching of the luminescence; possible reasons for this behaviour are discussed. The crystal structures of the two related complexes $[Ru(^tBu_2bipy)_2(L^1)][PF_6]_2$ and $[Cl_2Pt(\mu\text{-}L^2)Ru(bipy)_2][PF_6]_2$ are also described to illustrate arguments about the conformations of L^1 and L^2.

Introduction

The complex $[Ru(bipy)(CN)_4]^{2-}$, which was first reported in 1986, is of particular interest as a luminophore with highly solvatochromic properties.[1] Its absorption and emission properties, and its Ru(II)/Ru(III) redox potential, vary over a wide range according to the extent to which the lone pairs at the termini of the cyanide ligands interact with either solvent molecules[2] or other molecules such as cationic polyammonium macrocycles.[3] As such it is of interest as a sensor, undergoing (for example) a pronounced colour change depending on the humidity of its environment.[4] However $[Ru(bipy)(CN)_4]^{2-}$ has not been used as a component of multinuclear complexes, in contrast to the $[Ru(bipy)_2(CN)_2]$ unit which (*via* bridging cyanide interactions) has been extensively used as a component of multichromophoric arrays which display inter-component photoinduced energy-transfer.[5,6] Whereas $[Ru(bipy)_2(CN)_2]$ has two equivalent peripheral binding sites and so can be used to form simple chain complexes, the presence of *four* such binding sites of two distinct symmetry types in $[Ru(bipy)(CN)_4]^{2-}$ means that attempts to prepare multinuclear complexes by metalation of a limited number of these peripheral sites in a controlled geometry are likely to be difficult.

In this paper we describe an alternative approach which will allow exploitation of the unusual properties of the $[Ru(bipy)(CN)_4]^{2-}$ chromophore in multinuclear complexes. We have used simple derivatives of the 2,2′-bipyridyl chelate which possess peripheral vacant binding sites; this allows preparation of $[Ru(bipy)(CN)_4]^{2-}$ derivatives which may be used subsequently to prepare higher nuclearity species *via* a 'complexes as ligands' approach. The complexes are $[Ru(L^1)(CN)_4]^{2-}$ and $[Ru(L^2)(CN)_4]^{2-}$ (Scheme 1), based on the known ligands 2,2′:4′,4″-terpyridine (L^1)[7] and 2,2′:3′,2″:6″,2‴-quaterpyridine (L^2).[8] We have used L^2 in particular as a bridging ligand in a variety of multinuclear complexes which show inter-component photoinduced energy-transfer.[9] An additional feature of the pendant pyridyl or bipyridyl binding sites is that they can undergo protonation such that the properties of the chromophore are pH dependent,[10] and we have used these same two ligands to prepare pH-sensitive derivatives of the more well-known $[Ru(bipy)_3]^{2+}$ chromophore.[11,12] The syntheses of the two mononuclear complexes and the pH dependence of their optical absorption and luminescence properties are described in this paper, and show some interesting results related to competing effects on the optical properties of protonation at pendant pyridyl sites, or at the cyanide sites.

We also describe a time-resolved infrared (TRIR) spectroscopic study of $[Ru(L^2)(CN)_4]^{2-}$, which allows the IR spectrum of its excited state to be determined. Such studies have been invaluable in characterising the excited states of chromophores

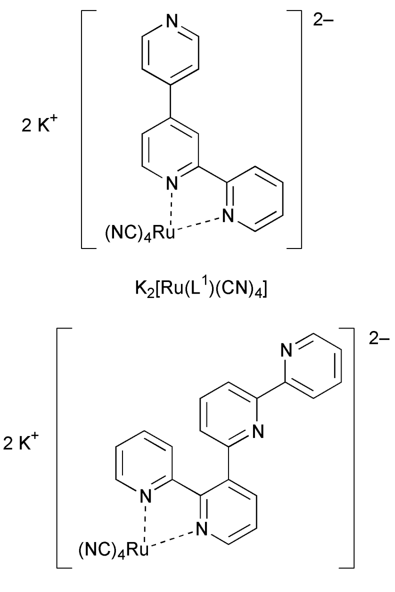

$K_2[Ru(L^1)(CN)_4]$

$K_2[Ru(L^2)(CN)_4]$

Scheme 1

which possess an obvious infrared 'reporter group' which is sensitive to the electron density on the metal centre,[13] notably Re(I)–carbonyl and Ru(II)–cyanide complexes, and have also been used to follow the inter-component energy-transfer processes in multinuclear complexes which contain an IR active chromophore.[6,14] The cyanide ligands of the $[Ru(bipy)(CN)_4]^{2-}$ unit are an ideal target for such a study.

Experimental

General details

The ligands L^1 (ref. 7) and L^2 (refs. 8, 9) were prepared as described previously. $K_4[Ru(CN)_6]\cdot 3H_2O$ was purchased from Johnson Matthey and used as received. Electrospray mass spectra of the complexes were recorded on aqueous solutions using a VG Quattro instrument, and FT-IR spectra on a Perkin-Elmer 1600 spectrophotometer.

Preparations

The syntheses of the two complexes described here are derived from a published method.[15]

$K_2[Ru(CN)_4(L^1)]$. A mixture of L^1 (0.233 g, 1 mmol) and $K_4[Ru(CN)_6]\cdot 3H_2O$ (0.467 g, 1 mmol) was suspended in MeOH–H$_2$O (20 cm^3, 1 : 1 v/v). This was acidified to a pH value of between 3 and 4 using aqueous H_2SO_4, and the mixture was then heated to reflux for 18 h after which time an orange precipitate had formed. On cooling, the mixture was neutralised with K_2CO_3 and the solvent was removed *in vacuo*. The residue was redissolved in water (3 cm^3) and filtered to remove any unreacted ligand L^1; the filtrate was then evaporated to dryness. The residue was dissolved in MeOH (50 cm^3) and unreacted $K_4[Ru(CN)_6]$ was then also filtered off. The solvent was then removed *in vacuo* and the residue was redissolved in the minimum amount of water. Addition of acetone (100 cm^3) precipitated the product as an orange solid in 40% yield; after filtration and washing with acetone the product was dried *in vacuo*. Negative-ion ESMS: *m*/*z* 516.3 {M}, 477.2 {M − K}, 439.3 {M − 2K}, 412.4 {M − 2K − CN}. IR (MeCN–D$_2$O, 1 : 1): ν_{CN} 2094, 2055, 2037 cm^{-1}. Found: C, 42.0; H, 2.6; N, 17.7. Required for $C_{19}H_{11}N_7RuK_2\cdot 1.5H_2O$: C, 42.1; H, 2.7; N, 18.0%.

$K_2[Ru(CN)_4(L^2)]$. This was prepared in exactly the same way from L^2 (0.100 g, 0.33 mmol) and $K_4[Ru(CN)_6]\cdot 3H_2O$ (0.151 g, 0.33 mmol) in H$_2$O–MeOH (60 cm^3, 1 : 1 v/v). The yield of material precipitated by addition of acetone to the final aqueous solution was 80%. Negative ion ESMS: *m*/*z* 554.5 {M − K}, 515.1 {M − 2K}, 489.0 {M − 2K − CN}, 462.1 {M − 2K − 2CN}. IR (MeCN–D$_2$O, 1 : 1): ν_{CN} 2094, 2056, 2039 cm^{-1}. Found: C, 44.2; H, 3.1; N, 17.0. Required for $C_{24}H_{14}N_8RuK_2\cdot 3H_2O$: C, 44.5; H, 3.1; N, 17.3%.

Time-resolved infrared spectroscopic studies

The Nottingham laser TRIR apparatus has been described in detail elsewhere.[16] In these experiments the excited state was produced by a pulsed Nd:YAG laser (Quanta-Ray GCR-12, 355 nm, 8 ns), and a cw IR diode laser (Mütek MDS 1100) was used to monitor the transient IR absorptions by means of a fast HgCdTe detector/preamplifier. The change in IR transmission at one particular IR frequency was measured following excitation and IR spectra were built up on a 'point-by-point' basis by repeating this measurement at different infrared frequencies.

Optical spectroscopic studies

Absorption spectra were recorded with a Perkin Elmer Lambda 9 Spectrophotometer in acetonitrile–water (1 : 1 v/v) solvent. Luminescence experiments were performed in the same solvent. Luminescence spectra were obtained from a Spex Fluorolog II spectrofluorimeter and uncorrected luminescence band maxima are used throughout the text. In order to determine luminescence quantum yields we employed corrected luminescence spectra on an energy scale (cm^{-1}). The corrected spectra were obtained by employing a calibrated 45-W quartz-halogen tungsten filament lamp by Optronic Laboratories as a standard for the correction of the phototube response. Luminescence quantum yields were then computed with reference to $[Ru(bipy)_3]Cl_2$ as a standard (Φ = 0.028 in air-equilibrated water),[17] as described previously.[9,11,12] Luminescence lifetimes were obtained with an IBH single-photon-counting apparatus whose thyratron-gated lamp was filled with N$_2$. Protonation experiments were carried out in acetonitrile–water solvent and titration with NaOH or HCl was employed to follow the spectroscopic changes. Use of HClO$_4$ gave identical results. The ionic strength during pH titrations was set at *ca.* 1 M by addition of KNO$_3$. The pH values employed throughout the text are *measured* values as read at a pH-meter by Hanna Instruments. The experimental uncertainty in the experimental band maximum both for absorption and emission is 2 nm, that for the luminescence intensity is 20%, and that for the lifetime is within 8%.

X-Ray crystallography

Crystals of $[Ru(^tBu_2bipy)_2(L^1)][PF_6]_2\cdot 1.5Et_2O\cdot Me_2CO$ (ref. 7) and $[Cl_2Pt(\mu\text{-}L^2)Ru(bipy)_2][PF_6]_2\cdot 2MeCN$ (ref. 18) were grown by diffusion of diethyl ether into concentrated solutions of the complexes in acetone or MeCN respectively. In each case a suitable crystal was coated with hydrocarbon oil and attached to the tip of a glass fibre, which was then transferred to a Siemens SMART diffractometer under a stream of cold N$_2$. Details of the crystal parameters, data collection and refinement for each of the structures are collected in Table 1. After data collection of a full sphere of data in each case an empirical absorption correction (SADABS) was applied,[19] and the structures were then solved by conventional direct methods and refined on all F^2 data using the SHELX suite of programs.[20] In all cases, non-hydrogen atoms were refined with anisotropic thermal parameters; hydrogen atoms were included in calculated positions and assigned isotropic thermal parameters. In both cases rapid loss of crystallinity occurred, associated with evaporation of solvent from the lattice during the mounting process; consequently the crystals diffracted rather weakly, and in each case only data below $2\theta = 45°$ were used in the final refinement. In each case the largest residual electron density peaks are close ($\approx$ 1 Å) to the heavy metal atoms.

Table 1 Crystallographic data[a]

Compound	$[Ru(^tBu_2bipy)_2(L^1)][PF_6]_2 \cdot 1.5Et_2O \cdot Me_2CO$	$[Cl_2Pt(\mu\text{-}L^2)Ru(bipy)_2][PF_6]_2 \cdot 2MeCN$
Empirical formula	$C_{60}H_{80}F_{12}N_7O_{2.5}P_2Ru$	$C_{44}H_{36}Cl_2F_{12}N_{10}P_2PtRu$
M_w	1330.32	1361.83
T/K	123(2)	173(2)
Crystal dimensions/mm	0.5 × 0.2 × 0.05	0.2 × 0.1 × 0.1
Crystal system, space group	Triclinic, $P\bar{1}$	Monoclinic, $P2_1/n$
a/Å	11.728(4)	10.791(2)
b/Å	16.034(6)	14.057(3)
c/Å	18.486(6)	31.308(5)
α/°	76.14(3)	90
β/°	81.46(5)	98.006(12)
γ/°	75.21(4)	90
V/Å^3	3249(2)	4702.8(14)
Z	2	4
D_c/g cm^{-3}	1.360	1.923
μ/mm^{-1}	0.372	3.569
Reflections collected: total/independent/R_{int}	22259/8486/0.1102	31350/6142/0.1175
Data/restraints/parameters	8486/141/792	6142/12/651
final R_1, wR_2[b,c]	0.0957, 0.2724	0.0708, 0.1402

[a] Data in common: λ = 0.71073 Å; Bruker SMART-CCD diffractometer. [b] Structure was refined on F_o^2 using all data; the value of R_1 is given for comparison with older refinements based on F_o with a typical threshold of $F \geq 4\sigma(F)$. [c] $wR_2 = [\Sigma[w(F_o^2 - F_c^2)^2]/\Sigma w(F_o^2)^2]^{1/2}$ where $w^{-1} = [\sigma^2(F_o^2) + (aP)^2 + bP]$ and $P = [\max(F_o^2, 0) + 2F_c^2]/3$.

CCDC reference numbers 167519 and 167520.

See http://www.rsc.org/suppdata/dt/b1/b105864a/ for crystallographic data in CIF or other electronic format.

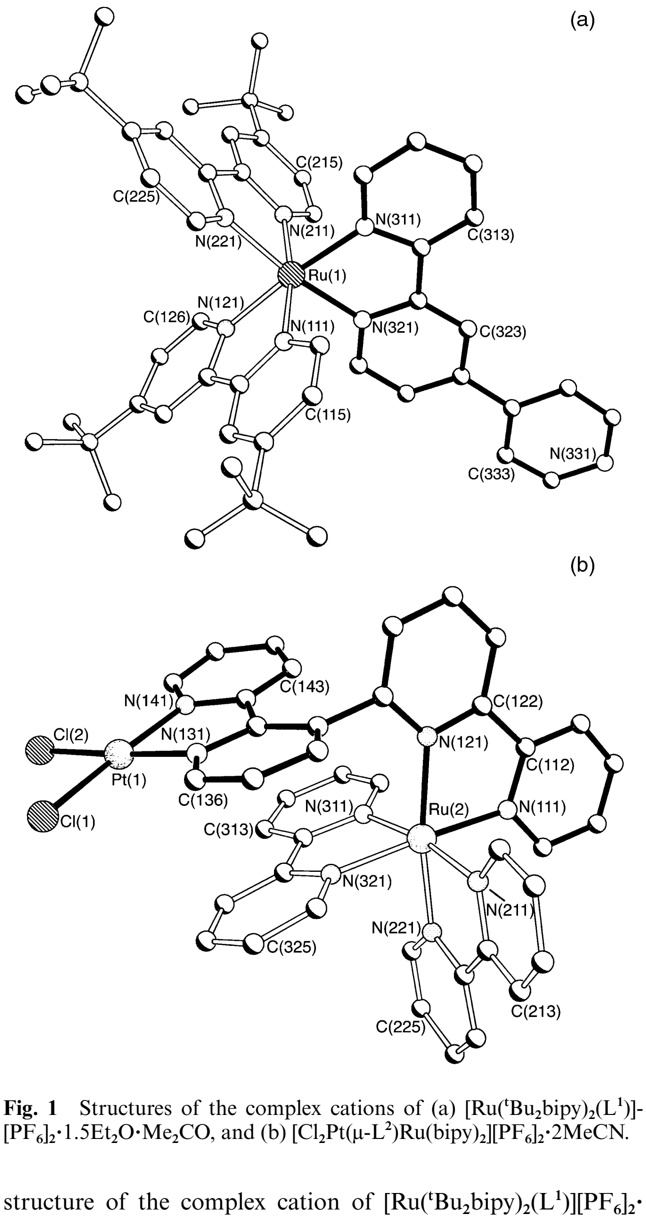

Fig. 1 Structures of the complex cations of (a) $[Ru(^tBu_2bipy)_2(L^1)][PF_6]_2 \cdot 1.5Et_2O \cdot Me_2CO$, and (b) $[Cl_2Pt(\mu\text{-}L^2)Ru(bipy)_2][PF_6]_2 \cdot 2MeCN$.

Results and discussion

Syntheses of new complexes, and crystal structures of two related complexes

The complexes were prepared by reaction of L^1 or L^2 respectively with $K_4[Ru(CN)_6]$ in aqueous acid at reflux (see Experimental section);[15] this is in contrast to the original photochemically-catalysed route for the preparation of $K_2[Ru(bipy)(CN)_4]$.[1] The identity of each complex was confirmed by negative-ion electrospray mass spectroscopy and elemental analysis. Solution IR spectra showed the presence of three cyanide stretching vibrations in each case, at very similar positions to those observed for $K_2[Ru(bipy)(CN)_4]$ under the same conditions.

In our earlier work where we examined the pH dependence of absorption and luminescence behaviour for the complexes $[Ru(bipy)_2(L^1)]^{2+}$ and $[Ru(bipy)_2(L^2)]^{2+}$, we found that they behaved quite differently as a result of the differing conformations of ligands L^1 and L^2.[11,12] We found that protonation of the pendant pyridyl site of $[Ru(bipy)_2(L^1)]^{2+}$ had a very strong effect on the complex, resulting in *e.g.* a substantial red-shift in the ^{1}MLCT absorption maximum and complete quenching of the emission,[12] whereas protonation of the pendant bipyridyl site of $[Ru(bipy)_2(L^2)]^{2+}$ resulted in much smaller perturbations of the optical properties.[11] This was ascribed to the fact that the pendant pyridyl unit of L^1 in $[Ru(bipy)_2(L^1)]^{2+}$ can be nearly coplanar with the coordinated bipy unit, such that there is strong electronic coupling between the two components.[7,12] In contrast, the conformation of L^2 is such that in $[Ru(bipy)_2(L^2)]^{2+}$ the pendant bipy unit is largely decoupled from the $\{Ru(bipy)_3\}^{2+}$ core because of a substantial twist between the free and coordinated bipy units of L^2.[9,11]

We expect the same factors to play a significant role in determining the pH dependence of the optical properties of $[Ru(L^1)(CN)_4]^{2-}$ and $[Ru(L^2)(CN)_4]^{2-}$ (see later). Although we could not isolate X-ray quality crystals of either of these new complexes, we present here the structures of two related complexes (both previously reported but not until now structurally characterised) which are relevant in that they illustrate the different conformational properties of the ligands L^1 and L^2 in their complexes (see Tables 1 and 2). Fig. 1(a) depicts the crystal structure of the complex cation of $[Ru(^tBu_2bipy)_2(L^1)][PF_6]_2 \cdot 1.5Et_2O \cdot Me_2CO$.[7] The structure of the $\{Ru(bipy)_3\}^{2+}$ core is unremarkable; the important point to note is the near-planarity

Table 2 Selected bond lengths (Å) and angles (°) for the two crystal structures

$[Ru(^tBu_2bipy)_2(L^1)][PF_6]_2\cdot1.5Et_2O\cdot Me_2CO$			
Ru(1)–N(211)	2.044(8)	Ru(1)–N(121)	2.061(8)
Ru(1)–N(321)	2.060(9)	Ru(1)–N(111)	2.059(9)
Ru(1)–N(221)	2.060(8)	Ru(1)–N(311)	2.070(9)
N(211)–Ru(1)–N(111)	170.9(3)	N(321)–Ru(1)–N(221)	172.3(3)
N(211)–Ru(1)–N(321)	97.3(3)	N(121)–Ru(1)–N(221)	89.7(3)
N(111)–Ru(1)–N(321)	89.3(3)	N(211)–Ru(1)–N(311)	89.7(3)
N(211)–Ru(1)–N(121)	94.6(3)	N(111)–Ru(1)–N(311)	97.7(3)
N(111)–Ru(1)–N(121)	78.4(4)	N(321)–Ru(1)–N(311)	78.3(4)
N(321)–Ru(1)–N(121)	96.8(3)	N(121)–Ru(1)–N(311)	173.8(3)
N(211)–Ru(1)–N(221)	78.0(3)	N(221)–Ru(1)–N(311)	95.5(3)
N(111)–Ru(1)–N(221)	96.0(3)		
$[Cl_2Pt(\mu\text{-}L^2)Ru(bipy)_2][PF_6]_2\cdot2MeCN$			
Ru(2)–N(311)	2.055(11)	Pt(1)–N(131)	2.015(10)
Ru(2)–N(221)	2.059(11)	Pt(1)–N(141)	2.020(11)
Ru(2)–N(321)	2.069(11)	Pt(1)–Cl(1)	2.286(4)
Ru(2)–N(111)	2.075(11)	Pt(1)–Cl(2)	2.302(3)
Ru(2)–N(211)	2.081(10)		
Ru(2)–N(121)	2.133(11)		
N(131)–Pt(1)–N(141)	80.8(4)	N(321)–Ru(2)–N(111)	173.8(5)
N(131)–Pt(1)–Cl(1)	95.7(3)	N(311)–Ru(2)–N(211)	170.4(5)
N(141)–Pt(1)–Cl(1)	176.5(3)	N(221)–Ru(2)–N(211)	78.8(4)
N(131)–Pt(1)–Cl(2)	176.4(3)	N(321)–Ru(2)–N(211)	93.9(4)
N(141)–Pt(1)–Cl(2)	95.7(3)	N(111)–Ru(2)–N(211)	89.4(4)
Cl(1)–Pt(1)–Cl(2)	87.77(14)	N(311)–Ru(2)–N(121)	89.9(4)
N(311)–Ru(2)–N(221)	93.8(4)	N(221)–Ru(2)–N(121)	170.9(4)
N(311)–Ru(2)–N(321)	78.9(5)	N(321)–Ru(2)–N(121)	106.6(4)
N(221)–Ru(2)–N(321)	82.3(4)	N(111)–Ru(2)–N(121)	78.0(4)
N(311)–Ru(2)–N(111)	97.1(5)	N(211)–Ru(2)–N(121)	98.3(4)
N(221)–Ru(2)–N(111)	93.2(4)		

of the ligand L^1, where there is a twist of just 5° between the pendant pyridyl units and the coordinated bipy unit of L^1. In the solid state this is in part due to packing effects; two adjacent complex molecules either side of an inversion centre are arranged such that the L^1 units stack efficiently (separation between stacked components, *ca.* 3.6 Å). This imposes a more planar conformation than is likely to exist in solution, but it is clear from this structure that L^1 can adopt a near-planar conformation which will facilitate electronic coupling between the pendant pyridyl unit and the $\{Ru(bipy)_3\}^{2+}$ core.

Fig. 1(b) depicts the crystal structure of the complex cation of $[Cl_2Pt(\mu\text{-}L^2)Ru(bipy)_2][PF_6]_2\cdot2MeCN$.[18] The structure is approximately as expected by comparison with other dinuclear complexes of L^2:[9] noteworthy points are the long bond Ru(2)–N(121) (see Table 2) which arises from the steric hindrance caused by the adjacent $\{Pt(bipy)Cl_2\}$ unit, and the intramolecular stacking between one of the bipyridyl ligands attached to the Ru(II) centre and the bipyridyl part of L^2 which is coordinated to the Pt(II) centre. The important point for the purposes of this paper is that, as with other complexes with L^2,[9] there is a near-orthogonal twist (89.5°) between the two bipy fragments of L^2 which will have the effect of minimising any electronic interactions between the two bipyridyl sites.

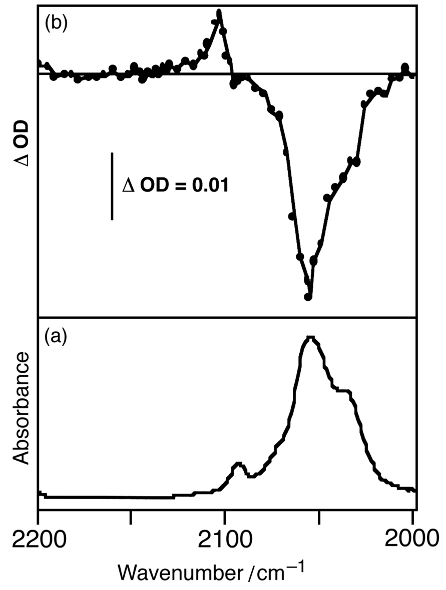

Fig. 2 Infrared spectra of $K_2[Ru(CN)_4(L^2)]$ in acetonitrile–D_2O (1 : 1): (a) in the ground state; (b) 30 ns after excitation at 355 nm (negative bands indicate depletion of starting material and positive bands are due to formation of a new species).

Time-resolved IR spectroscopy of $K_2[Ru(CN)_4(L^2)]$

Fig. 2(a) shows the ground state FTIR spectrum of a solution (10^{-2} M) of $K_2[Ru(CN)_4(L^2)]$ in acetonitrile–D_2O (1 : 1). Terminal ν(CN) IR bands appear at 2038, 2056 and 2093 cm^{-1} with the most intense peak being at 2056 cm^{-1}. Fig. 2(b) shows the time-resolved infrared spectrum obtained 30 ns after photolysis of this solution at 355 nm. The parent ν(CN) absorptions are bleached and a new band appears at 2104 cm^{-1}. This band can be assigned to the MLCT excited state in which the Ru^{II} centre has been oxidised to Ru^{III}; reduced Ru⟶CN back-bonding on transient oxidation of the metal results in a stronger C–N bond. The shift observed in the *ν*(CN) frequency from the ground to excited state (*ca.* +50 cm^{-1}) is similar to that observed by Bignozzi, Dyer, Meyer and co-workers in their TRIR spectrum of $[(phen)(CO)_3Re^I(NC)Ru^{II}(CN)(bipy)_2]^+$, in which the terminal *ν*(CN) stretch increased by 57 cm^{-1} in the $Ru^{II}\longrightarrow$bipy MLCT excited state.[21] The new absorption at 2104 cm^{-1} (corresponding to the MLCT excited state) decays at an identical rate [$k_{obs} = 2.6\ (\pm\ 0.3) \times 10^7\ s^{-1}$] to the recovery of the ground state bleach monitored at 2056 cm^{-1} [$k_{obs} = 2.5\ (\pm\ 0.3) \times 10^7\ s^{-1}$]. These data give a lifetime for the lowest-energy excited state of 38 ± 5 ns, in good agreement with the lifetime obtained from luminescence studies (see below). Unfortunately the complex $K_2[Ru(CN)_4(L^1)]$ was not sufficiently soluble to carry out similar experiments because of the relatively high concentrations required for these studies.

Table 3 Spectroscopic and photophysical data[a]

	Absorption		Emission				
	λ_{max}/nm ($10^{-3}\varepsilon$/dm^3 mol^{-1} cm^{-1})		λ_{max}/nm	$10^3\,\Phi$	τ/ns	$10^{-4}\,k_r$/s^{-1}	$10^{-7}\,k_{nr}$/s^{-1}
$[Ru(L^1)(CN)_4]^{2-}$	298 (14.8)	448 (4.6)	684	2.1	60	3.5	1.7
$[Ru(L^2)(CN)_4]^{2-}$	290 (22.7)	440 (3.0)	680	1.4	30	4.7	3.3
$[Ru(bipy)(CN)_4]^{2-}$, [b]	285 (27.3)	404 (4.1)	640				

[a] Solvent MeCN–water (1 : 1 v/v), room temperature. [b] In water, from ref. 2.

Optical spectroscopy

Table 3 collects absorption band maxima and intensities (λ_{max} and ε, respectively), and the luminescence band maximum (λ_{max}), quantum yield (Φ), and lifetime (τ) for $[Ru(L^1)(CN)_4]^{2-}$ and $[Ru(L^2)(CN)_4]^{2-}$, as obtained in air-equilibrated MeCN–water (1 : 1 v/v) solvent; the derived radiative and non-radiative rate constants, k_r and k_{nr}, respectively, for excited state deactivation are also listed in Table 3. The strong solvatochromism of Ru–polypyridine complexes containing the CN^- group is well documented[1–3,21,22] and, for comparison purposes, Table 3 also shows parameters obtained in water for $[Ru(bipy)(CN)_4]^{2-}$.[2] For the three complexes the identification of ^{1}LC transitions occurring in the spectral region 290–310 nm and of ^{1}MLCT transitions for the region 400–450 nm is straightforward. In the following sections we provide a detailed account of the absorption and emission properties of the examined complexes.

Titration of absorption spectra. Use of donating or accepting solvents, and the presence of cations, results in a strongly solvatochromic behaviour of complexes containing the CN^- group. Here, we have chosen to influence the spectroscopic properties of $[Ru(L^1)(CN)_4]^{2-}$ and $[Ru(L^2)(CN)_4]^{2-}$ *via* specific effects (protonation) at two distinct and spatially separate sites, *i.e.* the free N position of the pyridine rings of L^1 and L^2 on one hand, and of the CN^- groups on the other hand. In doing this, we have employed a titration approach by starting from basic MeCN–water solutions and titrating with HCl, and we can identify how different parts of the absorption spectrum will be affected by protonation at the two different sites.

The ligand protonation steps, occurring at the pendant pyridyl sites of L^1 and L^2, are expected to result in diagnostic changes in the UV portion of the absorption spectrum, the region of the ^{1}LC transitions. In contrast protonation of the CN^- groups would be expected to have relatively little effect on ^{1}LC transitions arising from L^1 or L^2. The spectral features of the visible region, *i.e.* the region pertaining to optical transitions of ^{1}MLCT character could be affected by protonation at *both* the pendant pyridyl sites and the CN^- sites. For the Ru⟶L^1 (and L^2) MLCT transitions, contrasting outcomes might be expected because (a) protonation at free pyridine should result in a lower lying MLCT level, depending on how strongly the pendant pyridyl unit is coupled to the $\{Ru(bipy)(CN)_4\}^{2-}$ core (as described above), whereas (b) protonation at one or more of the available CN^- groups should produce the opposite effect and will be independent of the conformation of L^1 or L^2.

Figs. 3 and 4 show ground state absorption spectra recorded for $[Ru(L^1)(CN)_4]^{2-}$ and $[Ru(L^2)(CN)_4]^{2-}$, respectively, at the indicated measured pH values. For both cases, isosbestic points are noted with changes occurring in two distinct regions, 290–340 nm (UV) and 400–500 nm (visible), which, as mentioned above, are due to transitions of ^{1}LC and ^{1}MLCT nature respectively.[23] For $[Ru(L^1)(CN)_4]^{2-}$, we have further plotted in Fig. 5(a) the absorbance changes against pH, as recorded at 296 nm (UV region), which are expected to arise only from protonation of L^1; the energy changes of the absorption maximum in the ^{1}MLCT region (visible) are illustrated in Fig. 5(b). From Fig. 5(a) we see that at pH < 5 the free N position of the pyridine ring of L^1 undergoes a protonation step, and from the inflection point of the sigmoid curve we find an apparent pK_a of 3.19 for this deprotonation–protonation equilibrium. It is interesting to note that the displacement of the MLCT maximum on going from basic to acidic solutions shows an oscillating behaviour, Figs. 3 and 5(b). In the pH interval 6–2.5, a stabilisation of the MLCT level by *ca.* 1000 cm^{-1} is observed, followed by a destabilisation of this level by more than 2000 cm^{-1} on going

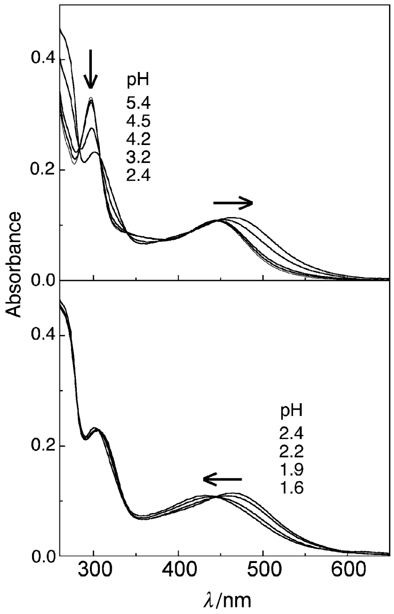

Fig. 3 Changes of the ground state absorption spectrum of $[Ru(L^1)(CN)_4]^{2-}$ (2.2×10^{-5} M solution) in MeCN–water (1 : 1, v/v) as a function of measured pH.

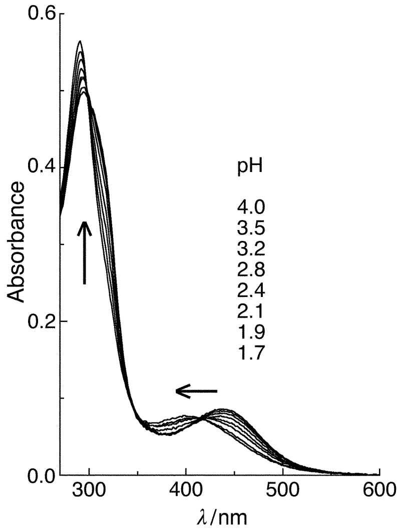

Fig. 4 Changes of the ground state absorption spectrum of $[Ru(L^2)(CN)_4]^{2-}$ (3.0×10^{-5} M solution) in MeCN–water (1 : 1, v/v) as a function of measured pH.

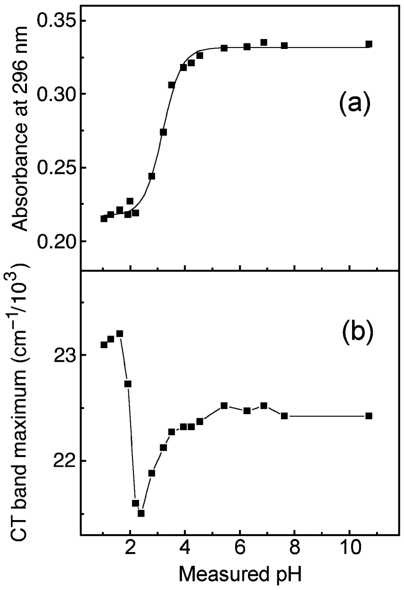

Fig. 5 Changes of (a) the absorbance at λ = 296 nm, and (b) the ^{1}MLCT absorption maximum, for $[Ru(L^1)(CN)_4]^{2-}$ (2.2 × 10^{-5} M solution) in MeCN–water (1 : 1, v/v) as a function of measured pH.

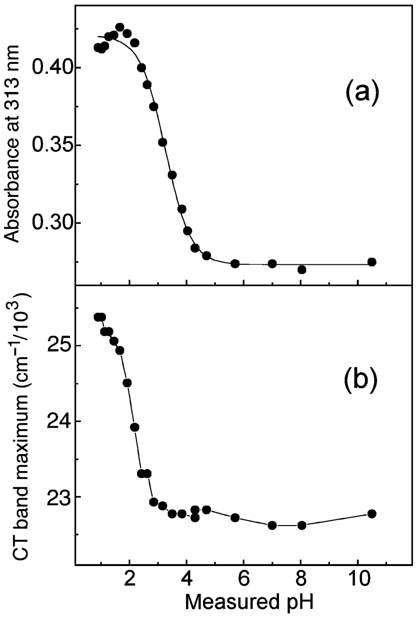

Fig. 6 Changes of (a) the absorbance at λ = 313 nm, and (b) the ^{1}MLCT absorption maximum, for $[Ru(L^2)(CN)_4]^{2-}$ (3.0 × 10^{-5} M solution) in MeCN–water (1 : 1, v/v) as a function of measured pH.

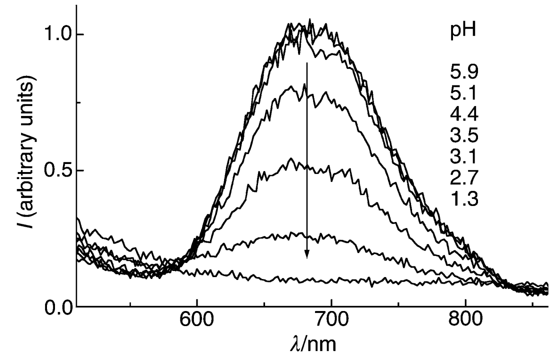

Fig. 7 Luminescence spectra of $[Ru(L^1)(CN)_4]^{2-}$ (2.2 × 10^{-5} M solution) in MeCN–water (1 : 1, v/v) as a function of measured pH; excitation was at the isosbestic point (308 nm).

from pH 2.5 to pH 1. These effects are related to the fact that the protonation steps expected at pyridine and at the CN^- groups are located at distinct (roughly 'opposite' with respect to the metal) spatial positions and are responsible for contrasting effects on the energy level of the MLCT transition, as described above. This allows us to separate the two protonation steps quite clearly, and from Fig. 5(b) we can see that protonation at CN^- occurs with an apparent pK_a of ≈ 2.

We note that the behaviour of $[Ru(L^1)(CN)_4]^{2-}$ is similar to that of the dicationic complex $[Ru(bipy)_2(L^1)]^{2+}$ as regards protonation at the pendant pyridyl group. For $[Ru(bipy)_2(L^1)]^{2+}$ the pK_a value for this protonation–deprotonation step was found to be 3.2 in water.[12] This is however not directly comparable to the value of 3.19 quoted above for $[Ru(L^1)(CN)_4]^{2-}$ because of the different solvent system used (for the current work, 1 : 1 MeCN–H_2O). This protonation resulted in stabilisation of the ^{1}MLCT state by 870 cm^{-1} for $[Ru(bipy)_2(L^1)]^{2+}$,[12] *cf.* ≈ 1000 cm^{-1} for $[Ru(L^1)(CN)_4]^{2-}$ [Fig. 5(b)].

The changes in absorbance at 313 nm (UV region) against pH for $[Ru(L^2)(CN)_4]^{2-}$, and the wavelength changes of the absorption maximum in the ^{1}MLCT region (visible region), are illustrated in Fig. 6(a) and 6(b), respectively. Again, we can separate protonation at the pendant bipy and at the CN^- sites because they have different effects on different parts of the absorption spectrum. Fig. 6(a) shows a sigmoidal curve with an apparent pK_a of 3.13, and since this relates to the ^{1}LC transition of L^2 we can assign this protonation–deprotonation equilibrium as based at the pendant bipy site of L^2. For $[Ru(bipy)_2(L^2)]^{2+}$ an apparent pK_a of ≈ 1.9 was determined for protonation at the bipy site,[11] which may be compared directly with the value of 3.13 found for $[Ru(L^2)(CN)_4]^{2-}$ because the same solvent system was used. The more facile protonation of $[Ru(L^2)(CN)_4]^{2-}$, by *ca.* 1.2 pK_a units, may be ascribed to a simple electrostatic effect arising from the negative charge on this complex.

In contrast to the behaviour seen with $[Ru(L^1)(CN)_4]^{2-}$, protonation of the bipy site of $[Ru(L^2)(CN)_4]^{2-}$ does not result in noticeable stabilisation of the ^{1}MLCT state; on going from basic to acidic conditions the ^{1}MLCT band maximum moves monotonically to *higher* energy (pH < 4), Fig. 6(b), due to protonation at the CN^- sites. The effect on the absorption spectrum in the ^{1}MLCT region due to protonation at the CN^- groups is clearly much greater than the effect arising from protonation of the opposite bipy periphery. This is ascribable to the spatial separation and the weak electronic coupling between the near-orthogonal coordinated and free bipy halves of L^2 as discussed above, and as we also observed for $[Ru(bipy)_2(L^2)]^{2+}$.[11] The fact that the changes in the ^{1}MLCT absorption maximum arise solely from protonation at the CN^- sites allows [from Fig. 6(b)] determination of an apparent pK_a of ≈ 2 for first protonation at the CN^- groups of $[Ru(L^2)(CN)_4]^{2-}$, essentially identical to the corresponding pK_a value of $[Ru(L^1)(CN)_4]^{2-}$ (above).

Titration of luminescence properties. The luminescence properties summarised in Table 3 are consistent with emission from a ^{3}MLCT excited state for both complexes.[23] The influence of pH on the luminescence of $[Ru(L^1)(CN)_4]^{2-}$ and $[Ru(L^2)(CN)_4]^{2-}$ has been monitored after excitation at convenient isosbestic points (λ_{exc} = 308 and 415 nm, respectively, see Figs. 3 and 4). Figs. 7 and 8 (showing luminescence spectra) and Figs. 9 and 10 (showing luminescence intensities and lifetimes), illustrate the luminescence results which are summarised here.

At measured pH values of >4, the luminescence intensity and band maximum for the ^{3}MLCT levels of both $[Ru(L^1)(CN)_4]^{2-}$ and $[Ru(L^2)(CN)_4]^{2-}$ exhibit no or small changes (Figs. 7 and 8, respectively), and the luminescence lifetimes are τ = 60 and 30 ns (±8%), respectively (Figs. 9 and 10); the value for $[Ru(L^2)(CN)_4]^{2-}$ is in reasonable agreement with a lifetime of 38 ± 5 ns determined from the TRIR studies on $[Ru(L^2)(CN)_4]^{2-}$. At these pH values neither the pendant pyridine

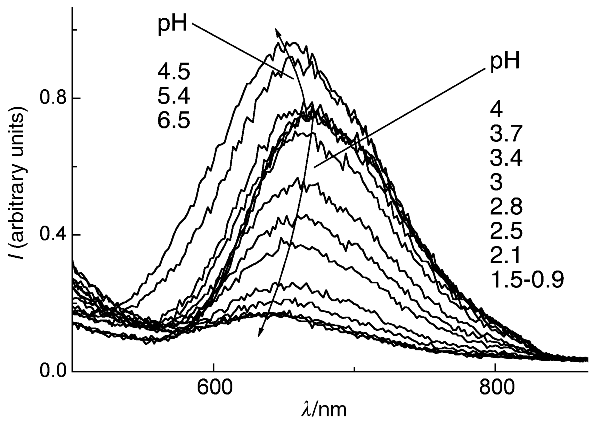

Fig. 8 Luminescence spectra of $[Ru(L^2)(CN)_4]^{2-}$ (3.0×10^{-5} M solution) in MeCN–water (1 : 1, v/v) as a function of measured pH; excitation was at the isosbestic point (415 nm).

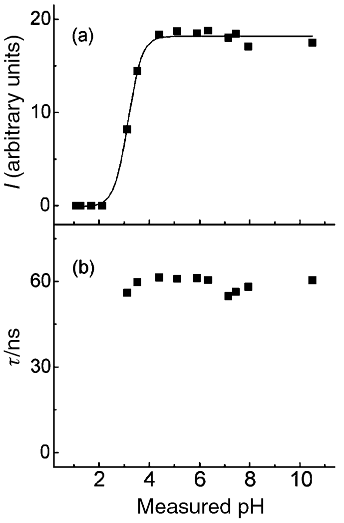

Fig. 9 Variations in (a) luminescence intensity, and (b) luminescence lifetime, for $[Ru(L^1)(CN)_4]^{2-}$ (2.2×10^{-5} M solution) in MeCN–water (1 : 1, v/v) as a function of measured pH; the inflection point of the upper curve is at pH 3.2.

sites nor the N atoms of the cyanide ligands are protonated and we observe the normal luminescent emission characteristic of the $\{Ru(bipy)(CN)_4\}^{2-}$ chromophore.

On changing the pH from 4 to 2, for both $[Ru(L^1)(CN)_4]^{2-}$ and $[Ru(L^2)(CN)_4]^{2-}$ the luminescence intensity is progressively quenched, with the values for τ remaining constant (Figs. 9 and 10). For $[Ru(L^1)(CN)_4]^{2-}$ the emission wavelength does not change as its intensity diminishes, (Fig. 7) whereas for $[Ru(L^2)(CN)_4]^{2-}$ the emission maximum undergoes a slight blue-shift as its intensity diminishes (Fig. 8). Plots of luminescence intensity *vs.* measured pH (Figs. 9 and 10) are sigmoid with the inflexion point—corresponding to 50% of the quenching—at a measured pH of 3.1 in each case. These values are essentially identical with the measured pK_a values for protonation of the pendant pyridyl or bipy sites of $[Ru(L^1)(CN)_4]^{2-}$ and $[Ru(L^2)(CN)_4]^{2-}$ respectively, indicating that quenching of the luminescence is associated with protonation at the pendant pyridine or bipy site in each case. The likely quenching mechanism is therefore photoinduced electron-transfer from the ^{3}MLCT excited state of the chromophore to the protonated pyridine which acts as an electron-acceptor; we note that *methylated* pyridines are well known as effective electron-accepting quenchers in this regard.[24] In addition, energy-transfer seems unlikely as there is no evidence that protonation of a pyridine results in new transitions having energies less than that of the excited-state of the $\{Ru(bipy)(CN)_4\}^{2-}$ chromophore.

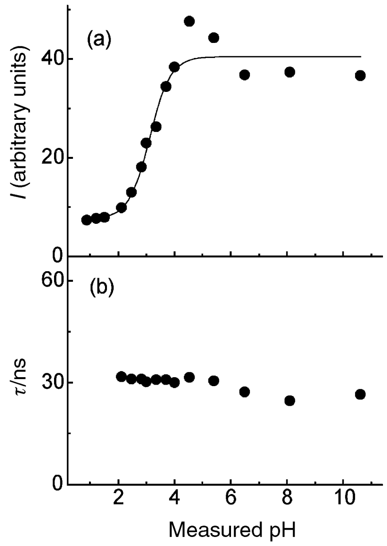

Fig. 10 Variations in (a) luminescence intensity, and (b) luminescence lifetime, for $[Ru(L^2)(CN)_4]^{2-}$ (3.0×10^{-5} M solution) in MeCN–water (1 : 1, v/v) as a function of measured pH; the inflection point of the upper curve is at pH 3.1.

The third possibility to account for the quenching—that it could be associated with the second protonation, at the CN^- sites—can also be ruled out in both cases because the inflexion point on the pH titration would have to be at pH ≈ 2 (the measured pK_a value for protonation at the CN^- sites). For $[Ru(L^1)(CN)_4]^{2-}$, the fact that the emission wavelength and lifetime are not affected as the emission intensity diminishes means that there is only a single luminescent species present during the titration, *i.e.* unprotonated $[Ru(L^1)(CN)_4]^{2-}$, in steadily decreasing amounts as the pH drops. If the pyridine-protonated species $[Ru(HL^1)(CN)_4]^-$ were also luminescent it would be expected to have a significantly lower emission wavelength, given the red-shift of 1000 cm^{-1} for the ^{1}MLCT absorption maximum on protonation of this complex (Fig. 3), but no such additional emission was detected. For $[Ru(L^1)(CN)_4]^{2-}$ all of the evidence is exactly consistent with complete quenching caused by the first protonation, at the pendant pyridyl unit, to give $[Ru(HL^1)(CN)_4]^-$.

For $[Ru(L^2)(CN)_4]^{2-}$ the situation is more complicated because the protonated species $[Ru(HL^2)(CN)_4]^-$ has residual luminescence which is slightly blue-shifted with respect to the un-protonated complex. The fact that quenching is not complete in this case can be explained by the relatively weak interaction between the pendant bipy site in $[Ru(L^2)(CN)_4]^{2-}$ with the complex core, such that the (presumed) photoinduced electron-transfer quenching by the protonated bipyridinium group is less effective. The fact that this residual emission of $[Ru(HL^2)(CN)_4]^-$ at low pH is blue-shifted compared to that of the non-protonated complex is consistent with protonation also occurring at the cyanide sites as shown by Scandola and co-workers.[25]

The observation that for both complexes in the pH interval 4–2 the luminescence intensity decreases while the lifetime τ is constant might be explained with reference to Scheme 2. Within this Scheme, the observed luminescence properties are only

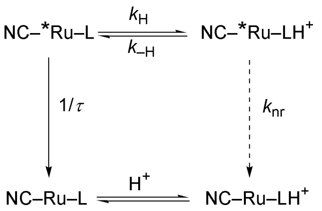

Scheme 2

ascribable to the unprotonated species **NC–*Ru–L** (where *Ru denotes the Ru centre in its excited state). In contrast, species that are protonated at the pendant pyridyl site **NC–*Ru–LH**$^+$, are taken to be non-emissive with highly effective non-radiative paths governing the deactivation of the excited state so that $k_{nr} \gg k_{-H}$.[26] This is accurate for $[Ru(L^1)(CN)_4]^{2-}$ but is only an approximation for $[Ru(L^2)(CN)_4]^{2-}$ which retains residual luminescence on protonation.

It is worth considering also the likely effects of protonation of the cyanide groups at lower pH values on the energy levels of these complexes. Due to electrostatic effects, protonation at cyanide is expected to destabilise the MLCT levels, and we have seen above that on going to lower and lower pH the ^{1}MLCT levels of $[Ru(L^1)(CN)_4]^{2-}$ and $[Ru(L^2)(CN)_4]^{2-}$ are raised in energy by *ca.* 1000 and 2000 cm^{-1} respectively [Figs. 5(b) and 6(b)]. As mentioned above, the blue-shift of the residual emission from $[Ru(HL^2)(CN)_4]^-$ can therefore be accounted for if there were also some protonation at one of the cyanide sites,[25] which is plausible given that the pK_a values for protonation at cyanide and at the pendant bipy group are quite close.

We also point out that, independently of the quenching route provided by protonation of pendant pyridyl residues in both complexes, protonation at the cyanide sites provides an additional and quite different deactivation pathway for the ^{3}MLCT excited state. Protonation of the CN$^-$ groups improves their ability to act as π-acceptors and decreases their ability to act as σ-donors; Scandola and co-workers showed that the result of these effects on the ^{3}MC and ^{3}MLCT energy levels for the similar complex $[Ru(bipy)_2(CN)_2]$ is to blue-shift the emission maximum and substantially reduce the emission quantum yield. We expect this effect to be operative for $[Ru(L^1)(CN)_4]^{2-}$ and $[Ru(L^2)(CN)_4]^{2-}$ at pH values (< 2.5) where the cyanide groups become protonated.

Conclusions

The complexes $[Ru(L^1)(CN)_4]^{2-}$ and $[Ru(L^2)(CN)_4]^{2-}$ contain the $[Ru(bipy)(CN)_4]^{2-}$ unit with pendant pyridyl or bipyridyl sites respectively; as such, they are suitable building-blocks for stepwise construction of polynuclear complexes in which their pronounced solvatochromism could be used as the basis of a switching action. Studies on the pH dependence of their absorption and emission spectra have shown that in acidic media, protonation can occur at both the pendant pyridyl sites (p$K_a \approx 3.1$) and at the externally-directed N atoms of the cyanide ligands (p$K_a \approx 2$), which have opposing effects on the energies of the MLCT excited state. The first protonation (at the pendant pyridyl sites) results in complete quenching of luminescence for $[Ru(L^1)(CN)_4]^{2-}$ and partial quenching of luminescence for $[Ru(L^2)(CN)_4]^{2-}$. The less effective quenching in the latter case is ascribed to the fact that the pendant bipyridyl site of $[Ru(L^2)(CN)_4]^{2-}$ is partly decoupled from the complex core by a substantial twist between the free and coordinated bipy fragments of L^2.

Acknowledgements

We thank the European Community (A. F. M., TMR contract no. CT98–0226; and COST Programme D11/0004/98), and the EPSRC (U.K.), for financial support.

Notes and references

1 C. A. Bignozzi, C. Chiorboli, M. T. Indelli, M. A. R. Scandola, G. Varani and F. Scandola, *J. Am. Chem. Soc.*, 1986, **108**, 7872; A. Ülveczky and A. Horváth, *Inorg. Chim. Acta*, 1995, **236**, 173.

2 C. J. Timpson, C. A. Bignozzi, B. P. Sullivan, E. M. Kober and T. J. Meyer, *J. Phys. Chem.*, 1996, **100**, 2915.

3 C. D. Borsarelli, S. E. Braslavsky, M. T. Indelli and F. Scandola, *Chem. Phys. Lett.*, 2000, **317**, 53; M. A. Rampi, M. T. Indelli, F. Scandola, F. Pina and A. J. Parola, *Inorg. Chem.*, 1996, **35**, 3355.

4 J. K. Evju and K. R. Mann, *Chem. Mater.*, 1999, **11**, 1425; C. E. Keller, C. Pollard, L. K. Yeung, W. D. Plessinger and C. J. Murphy, *Inorg. Chim. Acta*, 2000, **298**, 209.

5 C. A. Bignozzi, O. Bortolini, C. Chiorboli, M. T. Indelli, M. A. Rampi and F. Scandola, *Inorg. Chem.*, 1992, **31**, 172; F. Scandola, C. A. Bignozzi, C. Chiorboli, M. T. Indelli and M. A. Rampi, *Coord. Chem. Rev.*, 1990, **97**, 299; C. A. Bignozzi, S. Roffia, C. Chiorboli, J. Davila, M. T. Indelli and F. Scandola, *Inorg. Chem.*, 1989, **28**, 4350.

6 C. A. Bignozzi, R. Argazzi, C. Chiorboli, F. Scandola, R. B. Dyer, J. R. Schoonover and T. J. Meyer, *Inorg. Chem.*, 1994, **33**, 1652; C. A. Bignozzi, R. Argazzi, J. R. Schoonover, K. C. Gordon, R. B. Dyer and F. Scandola, *Inorg. Chem.*, 1992, **31**, 5260; K. Kalyanasundaram, M. Grätzel and M. K. Nazeeruddin, *Inorg. Chem.*, 1992, **31**, 5243.

7 M. A. Hayes, C. Meckel, E. Schatz and M. D. Ward, *J. Chem. Soc., Dalton Trans.*, 1992, 703.

8 M. D. Ward, *J. Chem. Soc., Dalton Trans.*, 1993, 1321.

9 D. A. Bardwell, F. Barigelletti, R. L. Cleary, L. Flamigni, M. Guardigli, J. C. Jeffery and M. D. Ward, *Inorg. Chem.*, 1995, **33**, 2438; V. Balzani, D. A. Bardwell, F. Barigelletti, R. L. Cleary, M. Guardigli, J. C. Jeffery, T. Sovrani and M. D. Ward, *J. Chem. Soc., Dalton Trans.*, 1995, 3601; R. L. Cleary, K. J. Byrom, D. A. Bardwell, J. C. Jeffery, M. D. Ward, G. Calogero, N. Armaroli, L. Flamigni and F. Barigelletti, *Inorg. Chem.*, 1997, **36**, 2601.

10 J. G. Vos, *Polyhedron*, 1992, **11**, 2285.

11 M. Guardigli, L. Flamigni, F. Barigelletti, C. S. W. Richards and M. D. Ward, *J. Phys. Chem.*, 1996, **100**, 10620.

12 A. M. W. Cargill Thompson, M. C. C. Smailes, J. C. Jeffery and M. D. Ward, *J. Chem. Soc., Dalton Trans.*, 1997, 737.

13 J. J. Turner, M. W. George, I. P. Clark and I. G. Virrels, *Laser Chem.*, 1999, **19**, 245.

14 J. R. Schoonover, A. Shreve, R. B. Dyer, R. L. Cleary, M. D. Ward and C. A. Bignozzi, *Inorg. Chem.*, 1998, **37**, 2598.

15 J.-L. Habib Jiwan, B. Wegewijs, M. T. Indelli, F. Scandola and S. E. Braslavsky, *Recl. Trav. Chim. Pays-Bas*, 1995, **114**, 542.

16 M. W. George and J. J. Turner, *Analyst*, 1994, **119**, 551.

17 K. Nakamaru, *Bull. Chem. Jpn.*, 1982, **55**, 2697.

18 A. M. Barthram, M. D. Ward, A. Gessi, N. Armaroli, L. Flamigni and F. Barigelletti, *New J. Chem.*, 1998, **22**, 913.

19 G. M. Sheldrick: SADABS, A program for absorption correction with the Siemens SMART area-detector system; University of Göttingen, 1996.

20 G. M. Sheldrick: SHELXS-97 and SHELXL-97 programs for crystal structure solution and refinement, University of Göttingen, 1997.

21 J. R. Schoonover, K. C. Gordon, R. Argazzi, W. H. Woodruff, K. A. Peterson, C. A. Bignozzi, R. B. Dyer and T. J. Meyer, *J. Am. Chem. Soc.*, 1993, **115**, 10996.

22 P. Belser, A. von Zelewsky, A. Juris, F. Barigelletti and V. Balzani, *Gazz. Chim. Ital.*, 1985, **115**, 723; F. Barigelletti, A. Juris, V. Balzani, P. Belser and A. von Zelewsky, *J. Phys. Chem.*, 1987, **91**, 1095; A. Juris, F. Barigelletti, V. Balzani, P. Belser and A. von Zelewsky, *J. Chem. Soc., Faraday Trans. 2*, 1987, **83**, 2295.

23 A. Juris, V. Balzani, F. Barigelletti, S. Campagna, P. Belser and A. von Zelewsky, *Coord. Chem. Rev.*, 1988, **84**, 85; T. J. Meyer, *Acc. Chem. Res.*, 1989, **22**, 163.

24 N. E. Katz, S. L. Mecklenburg and T. J. Meyer, *Inorg. Chem.*, 1995, **34**, 1282; R. J. Shaver, M. W. Perkovic, D. P. Rillema and C. Woods, *Inorg. Chem.*, 1995, **34**, 5446; M. Kropf, E. Joselevich, H. Dürr and I. Willner, *J. Am. Chem. Soc.*, 1996, **118**, 655; E. H. Yonemoto, R. L. Riley, Y. I. Kim, S. J. Atherton, R. H. Schmehl and T. E. Mallouk, *J. Am. Chem. Soc.*, 1992, **114**, 8081.

25 J. Davila, C. A. Bignozzi and F. Scandola, *J. Phys. Chem.*, 1989, **93**, 1373.

26 For **NC–*Ru–L** the occurrence of effective diffusion controlled protonation leading to **NC–*Ru–LH**$^+$ would be described by $\tau_o/\tau = I_o/I = 1 + k_q\tau_o[H^+]$, with $k_q = k_H/[1 + (k_{-H}/k_{nr})]$, see Scheme 2. The fact that the I_o/I behaviour is not paralleled by that for τ_o/τ suggests that diffusional processes *apparently* do not affect the luminescence of **NC–*Ru–L**; this may happen either for very slow ($1/\tau > k_H[H^+]$) or very fast ($1/\tau < k_H[H^+]$) protonation processes.